JOURNAL OF MATERIALS SCIENCE 31 (1996) 5009–5016

Decomposition of Al_2TiO_5–$MgTi_2O_5$ solid solutions: a thermodynamic approach

V. BUSCAGLIA, G. BATTILANA, M. LEONI
Istituto di Chimica Fisica Applicata dei Materiali-Consiglio Nazionale delle Ricerche, via De Marini 6, I-16149 Genoa, Italy
P. NANNI
Istituto di Chimica, Facoltà di Ingegneria, Fiera del Mare, Pad. D, I-16129 Genoa, Italy

The decomposition of $Al_{2(1-x)}Mg_xTi_{(1+x)}O_5$ solid solutions with $x = 0.0, 0.1, 0.2, 0.4, 0.5$ and 0.6 was studied in the temperature range 900–1175 °C using a 250 h annealing test. As x increases from 0–0.2 there is a strong stabilizing effect and the decomposition temperature decreases from 1280 °C (Al_2TiO_5) down to $\approx$ 1125 °C. For $0.2 \leqslant x \leqslant 0.5$ the decomposition temperature does not decrease further. For $x = 0.6$ no decomposition was observed. For $x \leqslant 0.5$ decomposition is complete or almost complete at 1000 °C; at 900 °C transformation is kinetically hindered and solid solutions with $x = 0.2$ and 0.4 are unaffected by the thermal treatment. A relationship between the decomposition temperature and the parameter x has been derived using the regular solution model to describe the $Al_{2(1-x)}Mg_xTi_{(1+x)}O_5$ solid solution.

1. Introduction

Sintered Al_2TiO_5 ceramics, owing to the high thermal expansion anisotropy of the individual grains [1], develop extensive microcracking along grain boundaries when the grain size exceeds a minimum critical value [2–5]. Such a microcracking takes place during cooling down from the sintering temperature and produces a material which exhibits an interesting combination of thermal properties [6] : very low thermal expansion coefficient ($1–1.5 \times 10^{-6}$ K^{-1}), low thermal conductivity (≈ 1.5 $W m^{-1} K^{-1}$) and excellent thermal shock resistance (≈ 500 $W m^{-1}$). For these reasons, Al_2TiO_5-based ceramics are promising candidate materials to be used in conditions involving severe thermal shocks, when good insulation is required: liners and manifolds of internal combustion engines, parts exposed to molten metals in metallurgy, thermal barriers. Al_2TiO_5 particles dispersed in dense ceramics can be used to improve both strength and toughness. Recently, alumina–aluminium titanate (20–30 vol%) composites with higher bending strength [7] and improved flaw tolerance [8] in comparison to pure alumina have been developed. Further applications for aluminium titanate are the coating of different materials by plasma spraying [9].

The poor mechanical properties of bulk Al_2TiO_5 [6] and the thermal instability below 1280 °C [10] constitute, however, a serious limitation to practical applications of this material. The first problem is directly related to microcracking, which results in the low thermal expansion but also in the low strength. Aluminium titanate composites with improved mechanical properties have been obtained by reaction sintering: Al_2TiO_5–mullite [11], Al_2TiO_5–$ZrTiO_4$–ZrO_2 [12], Al_2TiO_5–mullite–ZrO_2 [13].

The tendency to decompose in Al_2O_3 and TiO_2 is related to the thermodynamic instability of Al_2TiO_5 below 1280 °C [10]. The enthalpy of the reaction

$$\alpha - Al_2O_3 + TiO_2\text{–rutile} \rightarrow Al_2TiO_5 \quad (1)$$

is considerably positive [14] and formation of aluminium titanate becomes only feasible at high temperature because of the contribution of the configurational entropy arising from disordered distribution of Al^{3+} and Ti^{4+} on the cationic sublattice, as proposed by Navrotsky [15] and confirmed by Morosin and Lynch [16] from X-ray diffraction studies. The isostructural compound (orthorombic, pseudobrookite structure) Fe_2TiO_5 presents a similar behaviour and, in general, all pseudobrookite structures have a certain degree of substitutional disorder in the cationic sublattice [15, 17]. As a consequence, these compounds can be considered as “entropy stabilized” high-temperature phases. The Gibbs’ free energy of Reaction 1 has been calculated from the available thermodynamic data by Freudenberg and Mocellin [18] and results

$$\Delta G^0 = -10.95(\pm 3)(T - 1553)\,\mathrm{J\,mol^{-1}} \quad (2)$$

where T is the temperature (K). The decomposition of Al_2TiO_5 has been studied by various authors [19–22], both for sintered and powdered samples. The reaction kinetics is that of nucleation and growth and can be described using the Avrami model. The decomposition rate is maximum between 1100 and 1150 °C and decomposition is complete after 5–50 h, depending

0022–2461

on average grain size and annealing time above the decomposition temperature.

Decomposition of aluminium titanate can be controlled by MgO or Fe_2O_3 addition, which leads to the formation of solid solutions between Al_2TiO_5 and the isostructural compounds $MgTi_2O_5$ or Fe_2TiO_5 during sintering [23, 24]. The stabilizing effect is related to the improved thermodynamic stability of both $MgTi_2O_5$ and Fe_2TiO_5 in comparison with Al_2TiO_5. The compound $MgTi_2O_5$ decomposes in $MgTiO_3 + TiO_2$ below $\approx 700\,^\circ C$ [25, 26], whereas Fe_2TiO_5 decomposes in $Fe_2O_3 + TiO_2$ at $\approx 565\,^\circ C$ [15]. The most extensive study on the decomposition of Al_2TiO_5–$MgTi_2O_5$ solid solutions is that of Ishitsuka *et al.* [23]. The solid solutions, prepared by the mixed oxide route, present a complete range of solid solubility and can be described as $Mg_xAl_{2(1-x)}Ti_{(1+x)}O_5$, where two Al^{3+} ions are replaced by one Mg^{2+} ion and one Ti^{4+} ion. After 240 h annealing at 1100 °C, solid solutions with $x \leqslant 0.1$ were most decomposed, solid solutions with $0.2 \leqslant x \leqslant 0.6$ showed only limited decomposition (7%–15%), whereas compositions $x \geqslant 0.8$ remained unchanged. For the solid solution $x = 0.1$, no decomposition was observed at 1000 and 1200 °C. Some other papers deal with the decomposition of Al_2TiO_5 materials containing a limited amount of $MgTi_2O_5$ (10 mol%) [13, 27, 28]. In all cases, partial decomposition was observed between 1000 and 1150 °C. From the kinetic point of view, the presence of magnesium introduces a considerable delay before the decomposition starts, but the kinetics of the process is strongly influenced by the microstructure of the material. It has to be said that, even though considerable work has been carried out on the decomposition of Al_2TiO_5–$MgTi_2O_5$ solid solutions, some important points have not yet been completely investigated. In particular, decomposition products, decomposition temperature and long-term stability.

Decomposition products. Unlike Al_2TiO_5, in the case of solid solutions the presence of a magnesium-containing compound in the reaction products is required in addition to Al_2O_3 and TiO_2. The identification of such a compound will allow the decomposition reaction to be defined.

Decomposition temperature. Owing to the fragmentary nature of the investigations carried out in the past, the relationship between the amount of $MgTi_2O_5$ present in the solid solution and the corresponding decomposition temperature is unpredictable.

Long-term stability. On the basis of the currently available data, the long-term stability of Al_2TiO_5–$MgTi_2O_5$ materials in the temperature range 900–1200 °C is still an open question. This point is indeed of great importance in defining the maximum working temperature for practical applications.

In the present study a systematic investigation on the decomposition of Al_2TiO_5–$MgTi_2O_5$ solid solutions between 900 and 1175 °C is presented. The experimental results will be explained using a simplified thermodynamic model for the solid solution with the aim to define the relationship between the decomposition temperature and the composition.

2. Experimental procedure

Solid solutions $Mg_xAl_{2(1-x)}Ti_{(1+x)}O_5$ with composition corresponding to $x = 0, 0.1, 0.2, 0.4, 0.5$ and 0.6 were prepared using the mixed oxides route. Stoichiometric quantities of α-Al_2O_3 (Baikowski CR15, 99.99%, $X_{50} = 0.4\ \mu m$), TiO_2-rutile (Aldrich, 1317-80-2, 99.9%, $X_{50} = 1\ \mu m$) and MgO (Aldrich 34,279-3, 99%) were mixed by wet-milling with water and alumina balls in PE bottles for 24 h. MgO was treated, before mixing, for 8 h at 500 °C to decompose any $Mg(OH)_2$ possibly present. The resulting powders, after drying and sieving, were isostatically pressed at 150 MPa in the form of cylinders ($\approx$ 10 cm long, $\approx$ 1 cm diameter). The solid solutions were finally synthesized by reaction sintering at 1550 °C for 2 h. Decomposition tests were performed at different temperatures (900, 1000, 1100, 1125, 1150 and 1175 °C) for 250 h. Phase identification before and after annealing was performed by X-ray diffraction (XRD, Philips PW1050/PW1729/PW1710) using CoK_α radiation and a secondary graphite monochromator. The scanning step was 0.025 °2θ and the sampling time 5 s for each point, with digital collection of the resulting pattern. The quantitative phase composition of the annealed samples was obtained from the specific intensity of the reflections (0 2 3) of $Mg_xAl_{2(1-x)}Ti_{(1+x)}O_5$ and (1 1 0) of TiO_2–rutile by measuring the corresponding XRD peak area. The following system of linear equations was used

$$\frac{I_{ss}}{I_{TiO_2}} = C\frac{W_{ss}}{W_{TiO_2}} \tag{3a}$$

$$\frac{n_{MgAl_2O_4}}{n_{TiO_2}} = \frac{x}{1+x} \tag{3b}$$

$$\frac{n_{Al_2O_3}}{n_{TiO_2}} = \frac{1-2x}{1+x} \tag{3c}$$

$$W_{ss} + W_{TiO_2} + W_{Al_2O_3} + W_{MgAl_2O_4} = 1 \tag{3d}$$

where W_i is the weight fraction, n_i the number of moles, I_i the integral intensity and C is a constant dependent on the crystal structure and lattice parameters of titanate solid solution and rutile. Equation 3a follows from the general relationship between XRD intensity and composition [29], Equations 3b and c define the stoichiometric constraints corresponding to the decomposition reaction (see Equation 20 below) and Equation 3d represents the mass balance. The value of C, which depends on the composition of the solid solution, was calculated using the available crystallographic data [16] and the code Lazy-Pulverix [30] to compute some structural parameters. The measure of integral intensity was preferred over the measure of peak height to avoid effects arising from milling and annealing. The minimum detectable quantity of TiO_2 was $\approx$ 0.5 wt%. The decomposed fraction, β, of the annealed specimens was determined from the weight fraction of the different phases as

$$\beta = W_{Al_2O_3} + W_{TiO_2} + W_{MgAl_2O_4} = 1 - W_{ss} \tag{4}$$

Microstructure was observed by scanning electron microscopy (SEM, Philips 515) after infiltration of the samples in epoxy resin and usual metallographic preparation.

3. A simplified thermodynamic model for Al_2TiO_5–$MgTi_2O_5$ solid solutions

The regular solution model will be used to describe the thermodynamic properties of the Al_2TiO_5–$MgTi_2O_5$ solid solution. The solid solution is considered to be composed of three sublattices: the anionic sublattice formed by the O^{2-} ions and the cationic sublattices corresponding to the non-equivalent positions (4c) and (8f) detected from X-ray crystallography in the pseudobrookite-type structures. In the case of Al_2TiO_5, Al^{3+} and Ti^{4+} ions occupy the (8f) and (4c) sites, respectively. As the temperature increases, there is a tendency towards an increasing degree of disorder and the configuration of maximum entropy, i.e. complete random distribution, can be approached at high temperature, as argued by Navrotsky [15]. In agreement, Morosin and Lynch [16] observed no site preferences for the cations in Al_2TiO_5. The disorder of $MgTi_2O_5$ appears to vary continuously with temperature and becomes probably maximum above ≈ 1200 °C [17]. Complete disorder was found by high-resolution electron microscopy in the cation sublattice of Al_2TiO_5 and $Mg_{0.1}Al_{1.8}Ti_{1.1}O_5$ by Wohlfromm *et al.* [31]. It can then be reasonably assumed that a complete random distribution of Al^{3+}, Ti^{4+} and Mg^{2+} is present in the solid solution at high temperature. This assumption allows the configurational entropy of both the solid solutions and the two compounds to be calculated using the Temkin model.

3.1. Calculation of the entropy and enthalpy of mixing

The entropy of mixing, ΔS_m, can be expressed as

$$\Delta S_m = \Delta S_c + \Delta S_{nc}, \tag{5}$$

where ΔS_c is the configurational entropy and ΔS_{nc} the non configurational entropy. The configurational term ΔS_c will be considered to be the same as for an ideal solution. We will assume that the cations are randomly distributed over the cationic positions, whereas the anion sublattice is unaffected by mixing. Because the two compounds Al_2TiO_5 and $MgTi_2O_5$ have, in turn, a complete disordered cationic distribution, the expression of ΔS_c is

$$\Delta S_c = S_{c,SS} - S_{c,AT} - S_{c,MT} \tag{6}$$

where, for sake of brevity, the subscript AT indicates the compound Al_2TiO_5, the subscript MT the compound $MgTi_2O_5$ and the subscript SS the solid solution. The configurational entropy of the solid solution, $S_{c,SS}$, is

$$-\frac{S_{c,SS}}{R} = n_{Al}\ln\frac{n_{Al}}{\sum n_i} + n_{Ti}\ln\frac{n_{Ti}}{\sum n_i} + n_{Mg}\ln\frac{n_{Mg}}{\sum n_i} \tag{7}$$

where n_i is the number of moles of cations of kind i, and R the gas constant. The configurational entropy of the pure compounds is, accordingly,

$$-\frac{S_{c,AT}}{R} = n_{Al}\ln\frac{2}{3} + n_{Ti,AT}\ln\frac{1}{3} \tag{8}$$

$$-\frac{S_{c,MT}}{R} = n_{Ti,MT}\ln\frac{2}{3} + n_{Mg}\ln\frac{1}{3} \tag{9}$$

For 1 mol of solid solution, $n_{Mg} = x$, $n_{Al} = 2(1 - x)$ and $n_{Ti,AT} + n_{Ti,MT} = (1 + x)$, and Equation 6 becomes

$$-\frac{\Delta s_c}{R} = 2(1 - x)\ln(1 - x) + x\ln x + (1 + x)\ln(1 + x) - 2x\ln 2 \tag{10}$$

It should be noted that the same result can be obtained from the general expression of the configurational entropy of crystals containing several sublattices [32]

$$-\frac{S_c}{R} = \sum b^s N_i^s \ln N_i^s \tag{11}$$

where N_i^s is the fraction of species i in site s and b^s is the number of sites of types per formula unit, by maximization of S_c with respect to the N_i^s parameters.

The enthalpy of mixing for 1 mol of solid solution, Δh_m, can be calculated in the framework of the quasichemical approach to solutions. To do this, it will be assumed that the variation of enthalpy during mixing may be mainly attributed to a change in cation–cation interactions between nearest cation neighbours. Under this assumption it can be obtained (for derivation see Appendix)

$$\Delta h_m = x(1 - x)\omega \tag{12}$$

where ω is a parameter independent of temperature and composition.

The non-configurational part of the entropy of mixing, ΔS_{nc}, will be attributed only to a variation of vibrational entropy associated with cation–cation interactions. Following an identical argument to that just presented for the enthalpy of mixing, for one made of solid solution we obtain

$$\Delta s_{nc} = x(1 - x)\eta \tag{13}$$

where η is another parameter independent of temperature and composition.

The excess Gibbs' free energy of mixing for one mol of solid solution is then

$$g_m^E = x(1 - x)(\omega - \eta T) \tag{14}$$

and corresponds to the regular solution model.

3.2. Calculation of the components activity

From the definition of the chemical potential μ_i the activity of $Al_2l_iO_5$, μ_{AT}, results

$$\ln a_{AT} = \frac{\mu_{AT} - \mu^0_{AT}}{RT} = \frac{h_{AT} - h^0_{AT}}{RT} - \frac{s_{AT} - s^0_{AT}}{R}$$
$$= \frac{1}{RT}\left(\frac{\partial \Delta H_m}{\partial n_{AT}}\right)_{T,P,n_{MT}} - \frac{1}{R}\left(\frac{\partial \Delta S_{nc}}{\partial n_{AT}}\right)_{T,P,n_{MT}}$$
$$- \frac{1}{R}\left(\frac{\partial \Delta S_c}{\partial n_{AT}}\right)_{T,P,n_{MT}} \quad (15)$$

where h_i is the partial molar enthalpy, h^0_i the standard molar enthalpy, s_i the partial molar entropy and s^0_i the standard molar entropy of component i. After differentiation and substitution of Equations 12 and 13, Equation 15 becomes

$$\ln a_{AT} = -\frac{1}{R}\left(\frac{\partial \Delta S_c}{\partial n_{AT}}\right)_{T,P,n_{MT}} + \frac{1}{RT}(\omega - \eta T)x^2 \quad (16)$$

By inserting Equation 10 into Equation 16 and rearranging, we obtain the final expression for the activity of Al_2TiO_5

$$a_{AT} = (1 - x)^2(1 + x)\exp\left(\frac{\omega - \eta T}{RT}x^2\right) \quad (17)$$

Following an identical procedure, we obtain, for the activity of $MgTi_2O_5$

$$a_{MT} = \frac{1}{4}x(1 + x)^2\exp\left[\frac{\omega - \eta T}{RT}(1 - x)^2\right] \quad (18)$$

Equation 17 gives the activity of Al_2TiO_5 in the solid solution relative to the completely disordered pure Al_2TiO_5 as the standard state. Equation 18 has the same meaning referred to $MgTi_2O_5$. To reduce the number of parameters required to describe the solid solution, it is possible to introduce the approximation

$$(\omega - \eta T) = \theta \quad (19)$$

which holds when $\eta T \ll \omega$ or when the temperature variation is small. In the latter case, θ will represent the average value of $(\omega - \eta T)$ in the temperature range of interest.

The limitations of the proposed model are those typical of the regular solutions approach. In the calculation of the energy of mixing, only chemical contribution is taken into account. Pairwise interactions are assumed and the bonding energy is thus independent of composition. The contribution of stresses arising from the introduction of ions with different size in the lattice and the corresponding lattice deformation are neglected. The assumption of complete random distribution of cations in the present case is less critical and justified by the peculiar nature of the pseudobrookite-type compounds. The oxygen sublattice is considered to be unaffected by mixing; however, the O–O distances change with composition ($\approx 1\%$) giving a contribution to the energy of mixing.

4. Results and discussion

4.1. Results

The compositional dependence of the lattice parameters of $Mg_xAl_{2(1-x)}Ti_{(1+x)}O_5$ for $0.0 \leqslant x \leqslant 0.6$ is shown in Fig. 1. The values of a, b and c cell edges linearly change with x, indicating complete solid-state solubility between Al_2TiO_5 and $MgTi_2O_5$, in agreement with reported results [23]. Lattice parameters close to that reported on the JCPDS data base for $MgTi_2O_5$ [33] have been calculated by extrapolation of the data to $x = 1$ and, as a consequence, Vegard's law is obeyed. The sintering conditions (1550 °C, 2 h) were chosen to obtain single-phase, dense and large-grained materials. In fact the grain size is always > 10 μm and the final density $\geqslant 95\%$ of the theoretical value for all compositions, except the samples at $x = 0$, whose relative density is $\approx 85\%$. During cooling down, extensive microcracking along grain boundaries takes place. An example of the microstructure of the sintered material is shown in Fig. 2 for $x = 0.4$. The internal stresses originated by the anisotropy of the expansion coefficient should be completely released as, for grain size > 3–4 μm, they cannot be accommodated at the interior of grains and microcracking occurs [2–4].

The value of the decomposed fraction measured on the different samples is reported in Table I. Pure Al_2TiO_5 completely decomposes above 900 °C, whereas at the lowest temperature only a small amount

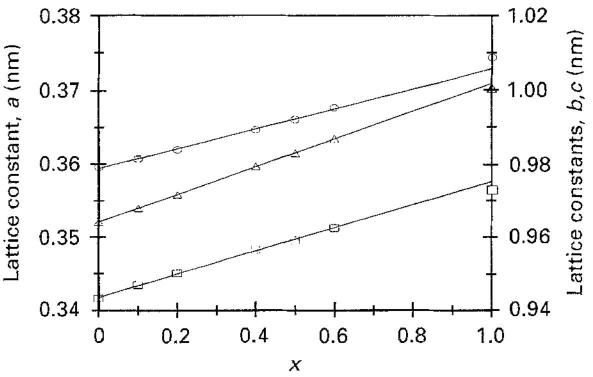

Figure 1 Compositional dependence of the lattice parameters (○) a, (□) b and (△) c of $Mg_xAl_{2(1-x)}Ti_{(1+x)}O_5$. Data corresponding to $x = 1$ from [33].

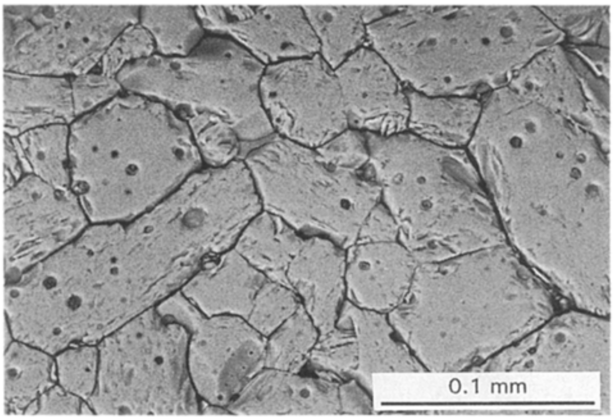

Figure 2 Microstructure of $Mg_{0.4}Al_{1.2}Ti_{1.4}O_5$ sintered 2 h at 1550 °C showing extensive microcracking along grain boundaries.

TABLE I Decomposed fraction of $Mg_xAl_{2(1-x)}Ti_{(1+x)}O_5$ after 250 h treatment at different temperatures

T (°C)	x					
	0	0.1	0.2	0.4	0.5	0.6
1175	1	0	0	0	0	0
1150	1	0.03	0	0	0.31	0
1125	1	0.96	0.01	0.08	1	0
1100	1	1	0.08	0.31	1	0
1000	1	1	0.72	1		0
900	0.84	0.1	0	0		0

(16%) of titanate is still present. Decomposition of the solid solution with $x = 0.6$ was not observed in the range 900–1175 °C. For $0.1 \leqslant x \leqslant 0.5$, the decomposition degree strongly depends on the annealing temperature. Solid solutions with $x = 0.2$ and 0.4 are stable at lower temperatures than those with $x = 0.1$ and $x = 0.5$; however, decomposition always occurs for $x \leqslant 0.5$ when the temperature goes below 1125 °C. At 900 °C, the decomposition is reduced or even inhibited ($x = 0.2$ and 0.4), probably because of kinetic effects.

The decomposition products, according to the phases detected by XRD, consist of TiO_2–rutile, α-Al_2O_3 and $MgAl_2O_4$–spinel for $x > 0$. The composition of the residual solid solution is that of the original one within the limits of XRD accuracy. As a consequence, the decomposition reaction can be written as

$$Mg_xAl_{2(1-x)}Ti_{(1+x)}O_5 \rightarrow xMgAl_2O_4 + (1-2x)Al_2O_3 + (1+x)TiO_2 \quad (0 \leqslant x \leqslant 0.5) \tag{20}$$

When $x = 0.5$, spinel and rutile are the only decomposition products. At larger values of x, if decomposition occurs, Equation 20 will no longer be appropriate to describe decomposition, as a new magnesium-containing phase has to appear on the right-hand side in place of Al_2O_3 to satisfy the mass balance.

Some attempts were made to study the reverse of Reaction 20, i.e. to determine the formation temperature of the solid solution versus composition. This was possible only in the case $x = 0.5$ and the reaction

$$\frac{1}{2}MgAl_2O_4 + \frac{3}{2}TiO_2 \rightarrow Mg_{0.5}AlTi_{1.5}O_5 \tag{21}$$

was found to proceed at temperatures $\geqslant 1175$° C, in agreement with the results of the decomposition tests. For $x < 0.5$, the composition of the solid solution depends both on temperature and the duration of the treatment even starting from the same initial mixture and reliable data cannot be easily obtained.

4.2 Calculation of the decomposition temperature

Equation 20 can be written as

$$xMgTi_2O_5 + (1-x)Al_2TiO_5 \rightarrow xMgAl_2O_4 + (1-2x)Al_2O_3 + (1+x)TiO_2 \tag{22}$$

and the corresponding equilibrium constant, K, is

$$\ln K = -\frac{\Delta G^0}{RT} = -x\ln a_{MT} - (1-x)\ln a_{AT} \tag{23}$$

where ΔG^0 is the standard Gibbs' free energy of reaction. The compounds TiO_2, $MgAl_2O_4$ and Al_2O_3 were assumed to be present as pure phases at unit activity. The value of ΔG^0 depends on temperature and composition; for the temperature range of interest (1000–1300 °C), the relationship

$$\Delta G^0 = A(x) + B(x)T \tag{24}$$

provides a good approximation to the values calculated from the available literature data [18, 25, 26]. The expressions for A and B are

$$A = -16927.7 + 9203.1x \quad \mathrm{J\,mol^{-1}} \tag{25}$$

$$B = 10.9 - 11.69x \quad \mathrm{J\,mol^{-1}\,K^{-1}} \tag{26}$$

Inserting Equation 17, 18 and 24 into Equation 23 and rearranging, we obtain the following expression for the decomposition temperature

$$T_d = \frac{A - \omega(x-x^2)}{R[x\ln(x/4) + 2x\ln(1+x) + (1-x)\ln(1+x) + 2(1-x)\ln(1-x)] - \eta(x-x^2) - B} \tag{27a}$$

Introduction of Equation 19, yields the alternative expression

$$T_d = \frac{A - \theta(x-x^2)}{R[x\ln(x/4) + 2x\ln(1+x) + (1-x)\ln(1+x) + 2(1-x)\ln(1-x)] - B} \tag{27b}$$

The above equations can be used to obtain the values of ω and η, or θ, which provide the best agreement, in the sense of least squares, between the model and the experimental data by an appropriate fitting procedure. A set of data couples (composition–decomposition temperature) was obtained by interpolation from the data of Table I. Because the partial derivatives of Equations 27a and b with respect to the parameters ω, η and θ contain the parameters themselves, a non-linear fitting technique has to be used. The method of Levenberg–Marquardt [34] is widely employed and can be considered as a standard of non-linear least-squares routines. Application of Equation 27a results in positive and very large values of both ω and η which produce a good fit, but have scarce physical meaning. On the other hand, application of Equation 27b produces a comparable good fit corresponding to $\theta = 33430 \pm 1000\ \mathrm{J\,mol^{-1}}$.

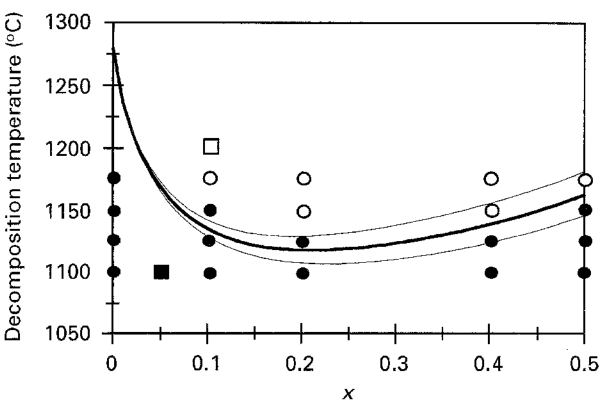

Figure 3 Decomposition temperature of $Mg_xAl_{2(1-x)}Ti_{(1+x)}O_5$ ($x \leqslant 0.5$) calculated from Equation 27b for $\theta = 33430\ \mathrm{J\,mol^{-1}}$ (——). (—) Variation of $\pm 1000\ \mathrm{J\,mol^{-1}}$ from the previous value. (●, ■) samples where decomposition was detected; (○, □) samples unaffected by the thermal treatment. (○, ●) Present work, (□, ■) [23].

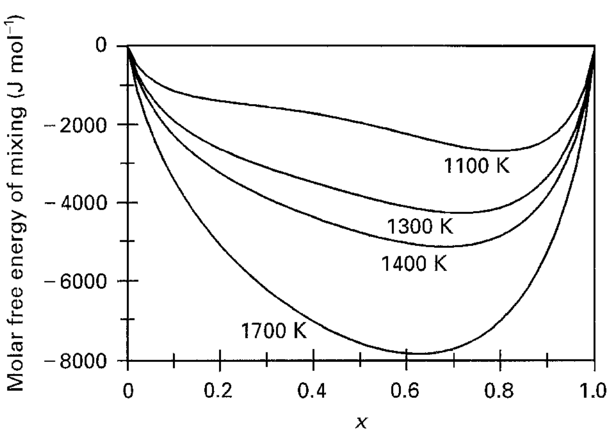

Figure 4 The molar Gibbs' free energy of mixing of $Mg_xAl_{2(1-x)}Ti_{(1+x)}O_5$ calculated at different temperatures.

As the expression of the total free energy of mixing is

$$\Delta g_m = - T\Delta s_c + g_m^E \qquad (28)$$

a positive value of θ implies a positive contribution of the excess free energy (Equation 14) to the free energy of mixing and hence a positive deviation from ideality. The decomposition temperature computed using the optimized value of θ is shown in Fig. 3 together with the data of Table I and from Ishitsuka *et al.* [23]. The model corresponding to Equation 27b provides a fair description of the experimental data, and, in particular, of the non-monotonic behaviour of the decomposition temperature versus composition. The fast decrease of the decomposition temperature when $x \leqslant 0.1$ is related to the stabilizing effect arising from the configurational entropy of mixing. As x further increases, the effect of the excess Gibbs' free energy of mixing (Equation 14) prevails and the decomposition temperature no longer decreases. The free energy of mixing computed from Equation 28 is shown in Fig. 4 for different temperatures. With the current value of the parameter θ, demixing of the solid solution is predicted below ≈ 1000 °C. Such a demixing is not experimentally observed even with cooling rates of 1 °C min^{-1}. Different explanations for this behaviour are possible:

(i) the present model is too approximate or inadequate to describe the solid solution below ≈ 1000 °C as partial ordering might occur;

(ii) the value of θ decreases as temperature decreases; this happens when in Equation 19 both ω and η are positive;

(iii) the demixing is inhibited by kinetic reasons: cation diffusion is known to be very slow [35] in Al_2TiO_5.

5. Conclusions

The decomposition of $Al_{2(1-x)}Mg_xTi_{(1+x)}O_5$ solid solutions with $x = 0.0$, 0.1, 0.2, 0.4, 0.5 and 0.6 was studied in the temperature range 900–1175 °C using a 250 h annealing test. The experimental results lead to the following conclusions.

1. As the value of x increases from $x = 0.0$ (pure Al_2TiO_5) to 0.2, the decomposition temperature accordingly decreases from 1280° C to ≈ 1125 °C. The presence of $MgTi_2O_5$ has a strong stabilizing effect on the solid solution.
2. For $0.2 \leqslant x \leqslant 0.5$ the decomposition temperature does not further decrease or even increases ($x = 0.5$).
3. For $x = 0.6$ decomposition was not observed in the whole range of temperature.
4. At 1000 °C decomposition is always complete or almost complete for $x \leqslant 0.5$.
5. At 900 °C decomposition is kinetically hindered and solid solutions with $x = 0.2$ and 0.4 are unaffected by the thermal treatment.

A relationship between the decomposition temperature and the parameter x has been derived using the regular solution approach to describe the $Al_{2(1-x)}Mg_xTi_{(1+x)}O_5$ solid solution. This model provides a fair description of the experimental data and in particular, predicts correctly the presence of a minimum in the decomposition temperature versus composition.

From the point of view of practical applications only the solid solution with $x = 0.6$ is stable at all temperatures between 900 and 1280 °C. However, the thermal stability should be tested for times longer than 250 h to assess the effective reliability of such a material in potential applications. Among the Al_2TiO_5 richer materials, the composition with $x = 0.2$ offers a better thermal stability, but prolonged exposure to temperatures in the range 900–1100 °C should be avoided in any case.

Acknowledgements

The authors thank Baikowski Chemie-Jocam s.r.l, Milan (Italy) for kindly providing the CR15 alumina powder.

Appendix. Calculation of the enthalpy of mixing

For a condensed system and at ordinary pressure levels, the enthalpy can be assumed to be equivalent to the energy of the system, because the difference, the term PV, is usually negligible. The energy of the cation sublattice may be calculated as a sum of pairwise interactions between cations first neighbours

$$E = \sum_{s,r} (P^{sr}_{11}E^{sr}_{11} + P^{sr}_{22}E^{sr}_{22} + P^{sr}_{33}E^{sr}_{33} + P^{sr}_{12}E^{sr}_{12} + P^{sr}_{13}E^{sr}_{13} + P^{sr}_{23}E^{sr}_{23}) \qquad \text{(A1)}$$

where the sum is extended to the different existing sites (s = 4c, r = 8f in the pseudobrookite-type structure). P^{sr}_{ij} represents the number of bonds between ions i and j located on the sites s and r, respectively. E^{sr}_{ij} is the corresponding bonding energy. For brevity, we will indicate aluminium by the index 1, magnesium by the index 2, and titanium by the index 3. Equation A1 is completely general and takes into account the presence of different sites in the lattice. As a consequence, for a given couple of first neighbour ions, the corresponding bonding energy will depend on the type of sites involved. The number of bonds is given by

$$P^{sr}_{ij} = N^s_i N^r_j n_s Z^{sr} \qquad \text{(A2)}$$

where N^s_i is the fraction of sites of type s occupied by atoms of type i, N^r_j is the fraction of sites of type r occupied by atoms of type j, n_s is the total number of sites of type s and Z^{sr} is the number of sites of type r first neighbours of sites of type s. By substitution of Equation A2 in Equation A1 we obtain

$$E = \sum_{s,r} n_s Z^{sr} \left(\frac{1}{2} N^s_1 N^r_1 E^{sr}_{11} + \frac{1}{2} N^s_2 N^r_2 E^{sr}_{22} + \frac{1}{2} N^s_3 N^r_3 E^{sr}_{33} + N^s_1 N^r_2 E^{sr}_{12} + N^s_1 N^r_3 E^{sr}_{13} + N^s_2 N^r_3 E^{sr}_{23} \right) \qquad \text{(A3)}$$

where the factor 1/2 arises from the fact that pairs involving the same kind of ions are counted twice in the summation. As we have assumed a complete random distribution, each cation will occupy the different sites with the same probability and hence $N^r_i = N^s_i = N_i$ and Equation A3 becomes

$$E = \frac{1}{2} N^2_1 \sum_{s,r} n_s Z^{sr} E^{sr}_{11} + \frac{1}{2} N^2_2 \sum_{s,r} n_s Z^{sr} E^{sr}_{22} + \frac{1}{2} N^2_3 \sum_{s,r} n_s Z^{sr} E^{sr}_{33} + N_1 N_2 \sum_{s,r} n_s Z^{sr} E^{sr}_{12} + N_1 N_3 \sum_{s,r} n_s Z^{sr} E^{sr}_{13} + N_2 N_3 \sum_{s,r} n_s Z^{sr} E^{sr}_{23} \qquad \text{(A4)}$$

and, introducing the composition variable x

$$N_1 = \frac{2}{3}(1 - x) \qquad \text{(A5a)}$$

$$N_2 = \frac{1}{3}x \qquad \text{(A5b)}$$

$$N_3 = \frac{1}{3}(1 + x) \qquad \text{(A5c)}$$

we finally obtain

$$E = \frac{4}{18}(1 - x)^2 \sum_{s,r} n_s Z^{sr} E^{sr}_{11} + \frac{1}{18} x^2 \sum_{s,r} n_s Z^{sr} E^{sr}_{22} + \frac{1}{18}(1 + x)^2 \sum_{s,r} n_s Z^{sr} E^{sr}_{33} + \frac{2}{9} x(1 - x) \sum_{s,r} n_s Z^{sr} E^{sr}_{12} + \frac{2}{9}(1 - x)(1 + x) \sum_{s,r} n_s Z^{sr} E^{sr}_{13} + \frac{1}{9} x(1 + x) \sum_{s,r} n_s Z^{sr} E^{sr}_{23} \qquad \text{(A6)}$$

Following an identical argument, it is possible to calculate the energy of the cationic sublattice of the two pure components

$$E_{\text{AT}} = \frac{4}{18} \sum_{s,r} {}^{AT}n_s Z^{sr} E^{sr}_{11} + \frac{1}{18} \sum_{s,r} {}^{AT}n_s Z^{sr} E^{sr}_{33} + \frac{2}{9} \sum_{s,r} {}^{AT}n_s Z^{sr} E^{sr}_{13} \qquad \text{(A7)}$$

$$E_{\text{MT}} = \frac{1}{18} \sum_{s,r} {}^{\text{MT}}n_s Z^{sr} E^{sr}_{22} + \frac{4}{18} \sum_{s,r} {}^{\text{MT}}n_s Z^{sr} E^{sr}_{33} + \frac{2}{9} \sum_{s,r} {}^{\text{MT}}n_s Z^{sr} E^{sr}_{23} \qquad \text{(A8)}$$

Assuming the oxygen sublattice to be unaffected by the mixing process, the energy of mixing can be simply obtained as $E - E_{\text{AT}} - E_{\text{MT}}$. For 1 mol of solution, as there are b_s sites of type s for each formula unit of solid solution, it is

$$n_s = b_s N_{\text{A}} \qquad \text{(A9a)}$$

$${}^{\text{AT}}n_s = (1 - x) b_s N_{\text{A}} \qquad \text{(A9b)}$$

$${}^{\text{MT}}n_s = x b_s N_{\text{A}} \qquad \text{(A9c)}$$

where N_{A} is Avogadro's number, and the final expression for the enthalpy of mixing of 1 mol of solid solution is

$$\Delta h_{\text{mix}} \simeq E - E_{\text{AT}} - E_{\text{MT}} = \frac{4}{18}(x^2 - x) \sum_{s,r} b_s Z^{sr} E^{sr}_{11} + \frac{1}{18}(x^2 - x) \sum_{s,r} b_s Z^{sr} E^{sr}_{22} + \frac{1}{18}(x^2 - x) \sum_{s,r} b_s Z^{s} E^{sr}_{33} - \frac{2}{9}(x^2 - x) \sum_{s,r} b_s Z^{sr} E^{sr}_{12} - \frac{2}{9}(x^2 - x) \sum_{s,r} b_s Z^{sr} E^{sr}_{13} + \frac{1}{9}(x^2 - x) \sum_{s,r} b_s Z^{sr} E^{sr}_{23} = x(1 - x)\omega \qquad \text{(A10)}$$

References

1. G. BAYER, *J. Less-Common Metals* **24** (1971) 129.
2. J. J. CLEVELAND and R. C. BRADT, *J. Am. Ceram. Soc.* **61** (1978) 478.
3. Y. OHYA, Z. NAKAGAWA and K. HAMANO, *ibid.* **70** (1987) C184.
4. F. J. PARKER and R. W. RICE, *ibid.* **72** (1989) 2364.
5. D. P. H. HASSELMAN, K. Y. DONALDSON, E. M. ANDERSON and T. A. JOHNSON, *ibid.* **76** (1993) 2180.
6. P. STINGL, J. HEINRICH and J. HUBER, in "Proceedings of the 2nd International Symposium on Ceramic Materials and Components for Engines", Lübeck-Travemünde (FRG), April 1986, edited by W. Bunk and H. Hausner (DKG, Bad Honnef, 1986) p. 369.
7. C.-S. HWANG, Z. NAKAGAWA and K. HAMANO, *J. Ceram. Soc. Jpn Int. Ed.* **102** (1994) 253.
8. N. P. PADTURE, S. J. BENNISON and H. M. CHAN, *J. Am. Ceram. Soc.* **76** (1993) 2312.
9. G. REHFELD, TH. STAUDT and C. ZOGRAFOU, *Ceram. Trans.* **1** (1988) 1100.
10. E. KATO, K. DAIMON and J. TAKAHASHI, *J. Am. Ceram. Soc.* **63** (1980) 355.
11. H. MOROSHIMA, Z. KATO, K. UEMATSU, K. SAITO, T. YANO and N. OOTSUKA, *J. Mater. Sci. Lett.* **6** (1987) 389.
12. F. J. PARKER, *J. Am. Ceram. Soc.* **73** (1990) 929.
13. H. WOHLFROMM, J. S. MOYA and P. PENA, *J. Mater. Sci.* **25** (1990) 3753.
14. M. S. J. GANI and R. McPHERSON, *Thermochim. Acta* **7** (1973) 251.
15. A. NAVROTSKY, *Am. Mineral.* **60** (1975) 249.
16. B. MOROSIN and R. N. LYNCH, *Acta Crystallogr.* **B28** (1972) 1040.
17. B. A. WECHSLER and A. NAVROTSKY, *J. Solid State Chem.* **55** (1984) 165.
18. B. FREUDENBERG and A. MOCELLIN, *J. Am. Ceram. Soc.* **70** (1987) 33.
19. T. KAMEYAMA and T. YAMAGUCHI, *J. Ceram. Soc. Jpn* **84** (1976) 589.
20. E. KATO, K. DAIMON and Y. KOBAYASHI, *ibid.* **86** (1978) 626.
21. E. KATO, Y. KOBAYASHI and K. DAIMON, *ibid.* **87** (1979) 81.
22. H. W. HENNICKE and W. LINGENBERG, *Ber DKG/CFI* **63** (1986) 100.
23. M. ISHITSUKA, T. SATO, T. ENDO and M. SHIMADA, *J. Am. Ceram. Soc.* **70** (1987) 69.
24. G. TILLOCA, *J. Mater. Sci.* **26** (1991) 2809.
25. G. ERIKSSON and A. D. PELTON, *Metall. Trans.* **24B** (1993) 795.
26. O. KNACKE, O. KUBASCHEWSKI and K. HESSELMANN, "Thermochemical properties of inorganic substances" (Springer, Berlin, 1991).
27. E. KATO, K. DAIMON, J. TAKAHASHI, R. KATO and K. HAMANO, Report of the Research Laboratory of Engineering Materials, Tokyo Institute of Technology, No. 9 (1984) 87, cited by H. A. J. Thomas and R. Stevens, *Br. Ceram. Trans. J.* **88** (1989) 184.
28. W. P. BYRNE, R, MORRELL and J. LAWSON, *Sci. Ceram.* **14** (1988) 775.
29. H. P. KLUG and L. E. ALEXANDER, "X-Ray Diffraction Procedures" (Wiley, New York, 1974) Ch. 7.2.
30. K. YVON, W. JEITSCHKO and E. PARTHE, *J. Appl. Crystallogr.* **10** (1977) 73.
31. H. WOHLFROMM, T. EPICIER, J. S. MOYA, P. PENA and G. THOMAS, *J. Eur. Ceram. Soc.* **7** (1991) 385.
32. H. ST. C. O'NEIL and A. NAVROTSKY, *Am. Mineral.* **68** (1983) 181.
33. JCPDS Powder Diffraction File, card 35–796 (International Centre for Diffraction Data, Swarthmore, USA, 1989).
34. W. H. PRESS, B. P. FLANNERY, S. A. TEUKOLSKI and W. T. VETTERLING, "Numerical Recipes" (Cambridge University Press, Cambridge, 1989) p. 521–8.
35. B. FREUDENBERG and A. MOCELLIN, *J. Mater. Sci.* **25** (1990) 3701.

Received 9 January
and accepted 18 March 1996